

β - Cyclodextrin / Carbon Xerogel Based Potentiometric Screen Printed Sensor for Determination of Meclofenoxate Hydrochloride

A.A. Abdul Aleem¹, Elmorsy Khaled^{2,*}, Ahmed A. Farghali³, Abdalla Abdelwahab³, M.M. Khalil¹

¹ Chemistry Department, Faculty of Science, Beni-Suef University, Beni-Suef, Egypt

² Microanalysis Laboratory, Applied Organic Chemistry Department, National Research Centre, El Bohouth St., Dokki, 12622 Giza, Egypt

³ Materials Science and Nanotechnology Department, Faculty of Postgraduate Studies for Advanced Sciences (PSAS), Beni-Suef University, 62511 Beni-Suef, Egypt

*E-mail: Elmorsykhaled@yahoo.com

Received: 23 November 2019 / Accepted: 26 January 2020 / Published: 10 March 2020

The present work described the fabrication protocol of disposable screen printed sensors for the potentiometric determination of meclufenoxate hydrochloride (MFX). Incorporation of the carbon xerogel (CG) as transducer, and (2,3,6-tri-O-methyl)-beta-cyclodextrin as molecular recognition elements in the electrode matrix improved the sensor performance. Comprehensive studies were performed on the sensing membrane components including; the nature of the sensing material, additives, plasticizers and nanomaterials. Improved sensitivity and selectivity were achieved in the MFX concentration ranged from 10^{-6} to 10^{-2} mol L⁻¹ with Nernstian compliance 62.7 ± 0.9 mV decade⁻¹. Addition of carbon gel as a novel carbon nanomaterial within the electrode matrix enhanced the potential reading stability, response time (< 4s) and prolonged lifetime of the fabricated sensors (5 months). Flow injection analysis (FIA) offers the advantages of automation feasibility, accuracy and high sampling output. The developed sensors were successfully applied for analysis of MFX in presence of its degradation products with agreeable average recoveries compared with the official methods.

Keywords: Carbon Xerogel; β - Cyclodextrin; Screen-printed potentiometric sensors; Meclofenoxate hydrochloride; Pharmaceutical samples

1. INTRODUCTION

Meclofenoxate (MFX, 4-chlorophenoxy)-acetic acid 2 (dimethylamino) ethyl ester) is a well-known cerebral stimulant acting as a nootropic agent for the treatment symptoms of alzheimer's disease and senile dementia [1-3].

The widespread consumption of pharmaceutical formulations required an accurate, selective and reproducible analysis protocol for quality control of pharmaceutical compounds. Chromatographic [4-8] and spectrophotometric [9-11] techniques are the most popular techniques for MFX quantification.

Majority of these techniques include several sample pretreatments with expensive apparatus and skilled operators. Electroanalytical techniques, with their advantages of adequate sensitivity with considerable operation cost and short measurement time, are now well established technique for pharmaceutical analysis [12-15]. Meclofenoxate polyvinyl chloride (PVC) membrane sensors modified with MFX-TPB ion-associate [16] and carbon paste electrodes incorporated with MFX-PTA [17] were reported in literature. The reported sensors showed cationic Nernstian responses in the MFX concentration ranged from 10^{-5} to 10^{-2} mol L⁻¹. More recently [18], our research team fabricated carbon paste electrode based on β -cyclodextrin/carbon and TiO₂ nanotubes for potentiometric determination of MFX. Improved performance with application for MFX determination in pharmaceutical products, spiked surface water and human urine samples with good recovery data was achieved.

Polyvinylchloride membrane and carbon paste potentiometric sensors are mechanically complicated with short operational lifetimes. These electrodes are inconvenient for biomedical analysis due to the difficulty of their miniaturization and the necessity for sterilization. More recently, large scale production of disposable planer screen printed electrochemical sensors with prolonged shelf-life was reported [19-26]. This methodology supports sensor miniaturization with portable devices and establishes its route from "lab-to-market" for a plethora of sensors.

The objective of the present study is to fabricate disposable sensors modified with a newly synthesized carbon xerogel/cyclodextrin/PVC nanocomposite for potentiometric determination of meclofenoxate.

2. EXPERIMENTAL PART

2.1. Reagents

Cyclic macromolecules including; the native α , β and γ - cyclodextrins (I-III), their methylated derivatives heptakis (2,6-di-O-methyl)- β -cyclodextrin (IV) and heptakis (2,3,6-tri-O-methyl)- β -cyclodextrin (V) were purchased from Sigma. In addition to cyclodextrin family, 12-crown-4 ether (VI, Fluka), 15-crown-5 ether (VII, Fluka), 18-crown-6 ether (VIII, Fluka), 21-crown-7 ether (IX, Fluka), dibenzo 24-crown-8 ether (X, Fluka), 30-crown- 10 ether (XI, Fluka), calix[4]arene (XII, Aldrich) and calix[8] arene (XIII, Aldrich) were tested as sensing ionophores.

Sodium tetraphenylborate (NaTPB, Fluka), sodium tetrakis (4-fluorophenyl) borate (NaTFPB, Sigma) and potassium tetrakis (4-chlorophenyl) borate (KTCIPB, Fluka) were applied as ionic additives. Plasticizers having different dielectric constants (ϵ) including; *o*-nitro phenyloctylether (*o*-NPOE, Sigma), 2-fluorophenyl 2-nitrophenyl ether (*f*-PNPE, Fluka), dioctylphthalate (DOP, Sigma), dioctylsebacate (DOS, Avocado) and tricresylphosphate (TCP, Fluka) were used. Poly (vinyl chloride)

(PVC, relative high molecular weight, Aldrich), graphite powder (synthetic 1– 2 μm , Aldrich) were used for fabrication of the printing ink.

Interferent solutions of Li^+ , NH_4^+ , Ca^{+2} , Mg^{+2} , Ni^{+2} , Co^{+2} , phosphate, citrate, maltose, starch, sucrose, glucose, fructose, glycine, caffeine and cysteine were prepared from analytical grade reagents and used for selectivity coefficient measurements.

2.2. Nanomaterials

Multi-wall carbon nanotubes (MWCNTs), single-wall carbon nanotubes (SWCNTs), graphene nanosheet (rG) were purchased from Sigma-Aldrich. Carbon nanotubes and TiO_2 nanotubes were synthesized as described elsewhere [18].

Nickel doped carbon xerogel (Ni-CX) was synthesized by the research team [27, 28]. Briefly, resorcinol and formaldehyde were dissolved in water with appropriate molar ratios. The molar ratio between resorcinol and formaldehyde was 1:2, while that between resorcinol and water was adjusted to be 1:17. The metal salt ($\text{Ni}(\text{CH}_3\text{COO})_2 \cdot 6\text{H}_2\text{O}$) acts as a catalyst for the polymerization reaction and in the same time as a dopant representing 6 wt.% of the final carbon structure. The obtained solution was poured in glass molds that held at temperature of 40 $^\circ\text{C}$ for 24 h, followed by maintaining at 80 $^\circ\text{C}$ for five days to complete the polymerization reaction. The obtained organic gel was dissolved in acetone for three days to perform the solvent exchange process, then dried in microwave to receive their corresponding organic xerogel. The organic xerogel was subjected to carbonization process at 900 $^\circ\text{C}$ for 2 h in nitrogen atmosphere with a heating rate of 5 $^\circ\text{C min}^{-1}$. Other studied carbon and metals nanoparticles were synthesized as described in details elsewhere [29-32].

2.3. Authentic samples and degradation product

Meclofenoxate hydrochloride authentic sample ($\text{C}_{12}\text{H}_{17}\text{Cl}_2\text{NO}_3$, 294.17 g mol^{-1}) was supplied by Mina Pharmaceutical Co., Cairo, Egypt, while its pharmaceutical preparation (Lucidril@250 mg) is purchased from local market.

The drug degradation products were prepared according to the procedure of El-Bardicy et al [16] using 2 mol L^{-1} sodium hydroxide at 100 $^\circ\text{C}$ for 25 min. After complete degradation, the reaction solution was acidified with HCl and the degradation products were then filtered and recrystallized from isopropyl alcohol.

The stock drug solution was prepared by dissolving the appropriate amount in bidistilled water. Working solutions covering the concentration range from 1×10^{-2} to 1×10^{-7} mol L^{-1} were freshly prepared by further dilution of the stock solution with bidistilled water.

2.4. Pharmaceutical preparation

Ten Lucidril tablets were weighed, grinded and an accurate weight of the powder equivalent to one tablet was dissolved in bidistilled water, filtered and completed to 50 mL with bidistilled water.

2.5. Biological fluids

Aliquots of urine sample (obtained from a donor healthy male) were spiked with MFX standard solutions, treated with 0.1 mL of 70% perchloric acid, vortexed for 1.0 min and centrifuged for 10 min. The supernatant was neutralized with NaOH and completed to 25 mL with water.

2.6. Apparatus

Metrohm 702 SM Titrino (Metrohm, Switzerland) was used for potentiometric and pH-measurements. SEM images were performed using Gemini Scanning Electron Microscope (SEM, Zeiss-Ultra 55) while HRTEM image was performed by JEOL-JEM. Surface area analysis was performed using N₂ gas adsorption at 77 K. Before analysis the sample was subjected for degassing at 110 °C for 2 h under helium atmosphere (TriStar II 3020, Micromeritics, USA). Flow injection manifold system composed of peristaltic pump (MCP Ismatec, Zurich, Switzerland) and sample injection valve (ECOM, Ventil C, Czech Republic) was constructed applying a continuous flow cells adapted for screen printed electrodes [33].

2.7. Procedures

2.7.1. Fabrication of sensors

Screen printed electrodes (5 × 35 mm) were printed using graphite-based inks as described in details elsewhere [34]. Following, the ion-sensing cocktail composed of 2.0 mg heptakis (2,3,6-tri-O-methyl)- β -cyclodextrin (V), 1.0 mg KTCIPB and 360 mg *f*-PNPE were dissolved in 6 mL THF followed by addition of 240 mg PVC and 10.0 mg carbon gel. After sonication for 30 min, the matrix cocktail was dropcasted on the graphite/PVC layer and left to dry at 50 °C. Prior potentiometric measurements, the printed sensors were preconditioned in 10⁻³ mol L⁻¹ MFX solutions for 20 min.

2.7.2. Sensors calibration

Under batch potentiometric mode, sensors were calibrated according the IUPAC recommendation by immersing the working and reference electrodes in different MFX solutions covering the concentration range from 10⁻⁷ to 10⁻² mol L⁻¹ at 25°C in ascending order [35]. Calibration graphs were constructed by plotting the potential readings against MFX concentrations in logarithmic scale. For FIA measurements, 50 μ L of freshly prepared drug solutions were injected in the flowing stream with flow rate of 12.6 mL min⁻¹ [33] and the corresponding peak heights were plotted against MFX concentration in logarithmic scale.

2.7.3. Potentiometric determination of MFX in pharmaceutical and biological samples

Under standard addition mode, small increments of the MFX standard solution were injected in the sample solution and the electrode potentials corresponding to each increment were used to estimate the MFX concentration in the sample solution [36]. Under the potentiometric titration, volumes of the MFX samples containing 1.29 to 1.29 mg MFX were titrated against standardized NaTPB solution applying the fabricated MFX sensor as indicator electrode [37]. For FIA measurements, the sample solutions were injected in the carrier stream and the peak heights were compared to those obtained from injection of MFX standard solutions of the same concentration. In all cases, the obtained recoveries were compared with the reported method [38].

3. RESULT AND DISCUSSION

3.1. Characterization of nanomaterial

The synthesized carbon xerogel showed high surface area (S_{BET}) equal to $663 \text{ m}^2\text{g}^{-1}$. In addition, the micropore volume (W_o) and the pore diameter (L_o) are equal to $0.26 \text{ cm}^3\text{g}^{-1}$ and 1.0 nm , respectively indicating that the Ni-CX contains both micro- and mesopores structure.

Table 1. Surface area analysis of Ni-CX

Sample	S_{BET} (m^2g^{-1})	W_o (cm^3g^{-1})	L_o (nm)
Ni-CX	663	0.26	1.0

The nickel doped carbon xerogel (Ni-CX) morphology was characterized by scanning electron microscopy (SEM). Spherical particles of carbon are connected together in a continuous network which is the normal morphology was observed (Fig.1a). The presence of porosity on the carbon xerogel surface which facilitate the solvent diffusion inside (Fig. 1b).

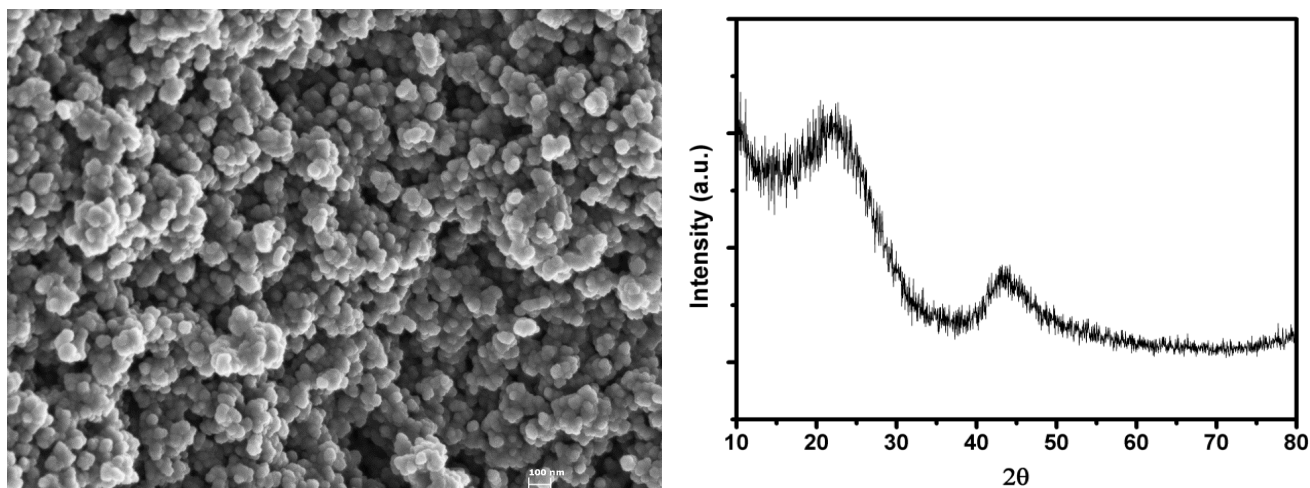


Figure 1. SEM image and XRD pattern of Ni-CX

3.2. Macromolecules as molecular recognition elements

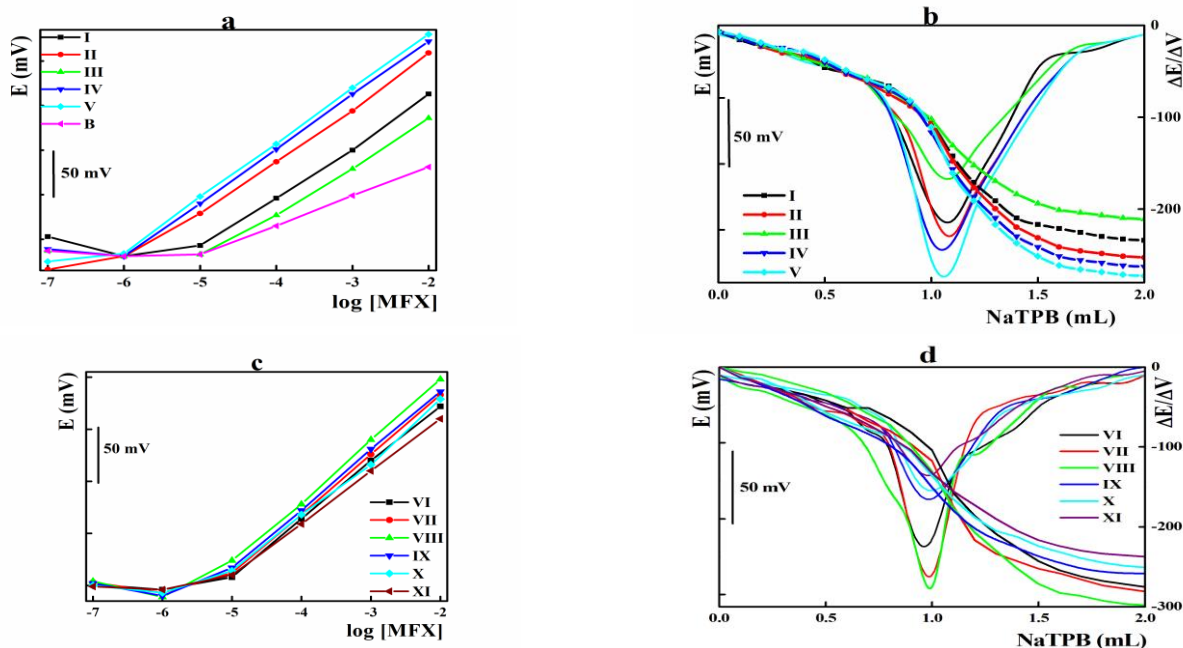
During the last decades, wide range applications of cyclodextrines were reported in analytical chemistry, biomedical and pharmaceutical analysis [39-43]. The interior CD cavity was lined with skeletal carbon and ether oxygen atoms of the glucopyranose which offer a microenvironment for fitting the nonpolar part of the guest molecule and formation of the inclusion complex. The formation of inclusion complex between molecular recognition and drug represents one of the promising approaches for improvement of the electroanalytical procedures. The formation of such inclusion complex depends on the size of both analyte and CD and spatial structure of the guest function groups.

3.3. Optimization of the sensor compositions

To achieve the highest sensor performance, several factors affecting the sensor performance such as the nature of sensing ionophores, anionic sites, plasticizers and nanomaterials were studied.

3.3.1. Effect of sensing ionophores

Dummy sensors fabricated without addition of the recognition element showed sub Nernstian slope (31.1 ± 1.1 mV decade⁻¹). Aiming to elucidate the rule of the molecular recognition element on the sensor performance, 13 different ionophore families including cyclodextrins, crown ethers and calixarenes were tested (**Fig.2**).



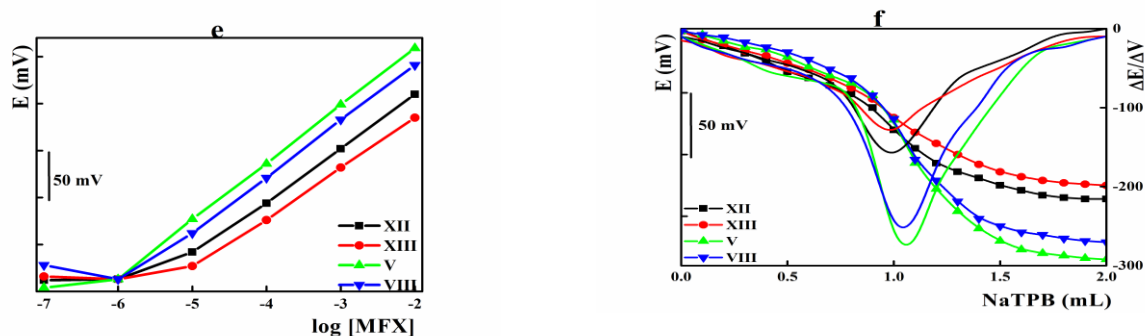


Figure 2. a, c, e) Effect of the ionophores on MFX sensor performance, b, d, f) potentiometric titration of 1 mL of 10^{-2} mol L $^{-1}$ MFX with 10^{-2} mol L $^{-1}$ NaTPB solution.

Among cyclodextrin family, the methylated β -CD (either 2,6-di-O-methyl- β -CD (IV) or 2,3,6-tri-O-methyl- β -CD (V)) showed the highest performance with cationic Nernstian compliance (60.5 ± 0.3 and 61.4 ± 0.4 mV decade $^{-1}$, respectively) compared with other cyclodextrin ionophores (Fig. 2a). Similar conclusion was obviously shown under the potentiometric titration modes using sensors incorporated with different cyclodextrin compounds where β -CD (V) was the most appropriate (Fig. 2b).

The potentiometric responses for β -CDs based sensors were in the following order; 2,3,6-tri-O-methyl- β -CD (V) > 2,6-tri-O-methyl- β -CD (IV) > β -CD (II). Even the tested three derivatives have the same cavity radii, the difference of the slope values (which is related to the stability constant of the formed inclusion complexes) may be attributed to improvement of the cavity height and effect of substitution with methyl derivatives on the hydrophobicity of the ring side. The un-substituted β -cyclodextrin showed ring height 8 $^{\circ}$ A, therefore, part of the meclufenoxate molecule may still be outside the nanocage (vide infra). Upon methylation, the ring height increased to 11 $^{\circ}$ A [44] with the improvement of the cavity hydrophobicity [45]. Thus, greater tendency of meclufenoxate towards substituted β -CD will enhance the penetration of MFX inside the ring cavity and increase the inclusion complex stability.

Crown ether structure showed a confirmation of a central cavity suitable for trapping the guest molecules [46]. Crown ethers form highly stable complexes with protonated amines and ammonium cation [47]. From different CE derivatives, 18-crown-6 ether (VIII), with cavity size suited for fitting MFX ions, showed highest sensitivity (58.4 ± 1.0 mV decade $^{-1}$, Fig. 2c). Selection of 18-crown-6 ether (VIII) was also sustained from the potentiometric titration data (Fig. 2d).

Moreover, the performances of sensors incorporated with β -CD compounds (V), 18-crown-6 ether (VIII), calixarene derivatives (XII, XIII) were represented graphically in (Fig. 2e & f). The obtained results suggested the β -CD for constructing MFX sensor.

3.3.2. Effect of ionic additives

Cyclodextrins are neutrally charged macromolecules, therefore, their potentiometric sensors operate only in the presence of anionic sites with an opposite charge to the target analyte. The function of ionic sites is attract analyte to the electrode surface and promote the ion exchange leading

to improvement in the selectivity and the sensitivity of the sensor [48-50]. In absence of charged anionic sites sub Nernstian response (about 27.7 ± 3.5 mV decade⁻¹) was recorded, while incorporation of the tetraphenylborates derivatives improved the performance to theoretical Nernstian response (53.2 ± 1.3 , 56.8 ± 0.7 and 58.2 ± 1.0 mV decade⁻¹ for NaTPB, NaTFPB and KTCIPB, respectively) (Fig. 3a). Potentiometric titration of MFX against NaTPB was performed using sensors contained the different tetraphenylborates derivatives and KTCIPB showed higher potential jump compared to the other electrodes (Fig. 3b).

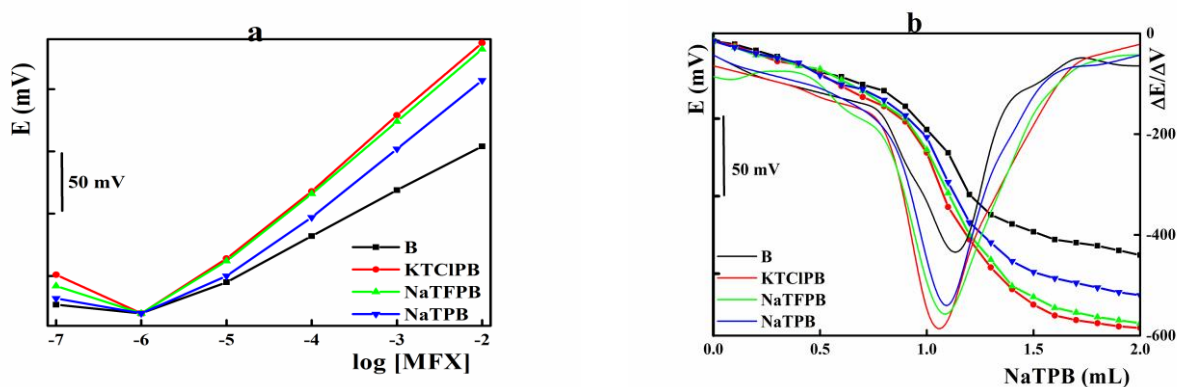


Figure 3. Effect of the ionic sites on: a) MFX sensor performance; b) potentiometric titration of 1 mL of 10^{-2} mol L⁻¹ MFX with 10^{-2} mol L⁻¹ NaTPB solution.

3.3.3. Effect of membrane plasticizer

The polarity of membrane plasticizers indicated by their dielectric constant governed the polarity of sensing membrane, mobility of the sensing ionophore and stability of the formed inclusion complex [50-52]. Herein, five different plasticizers were applied as solvent mediator namely, DOP, DOS, TCP, *o*-NPOE and *f*-PNPE (different dielectric constants values were 3.8, 5.2, 17.6, 24 and 50, respectively) [53].

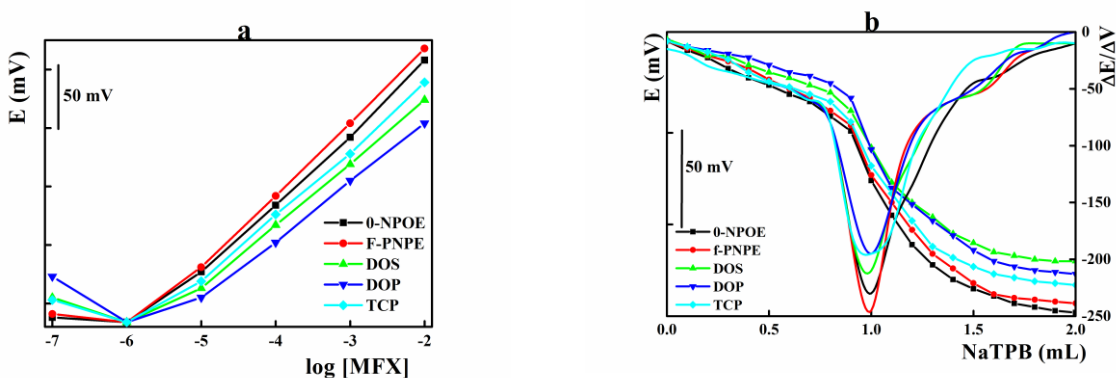


Figure 4. Effect of the membrane plasticizer on: a) MFX sensor performance; b) potentiometric titration of 1 mL of 10^{-2} mol L⁻¹ MFX with 10^{-2} mol L⁻¹ NaTPB solution.

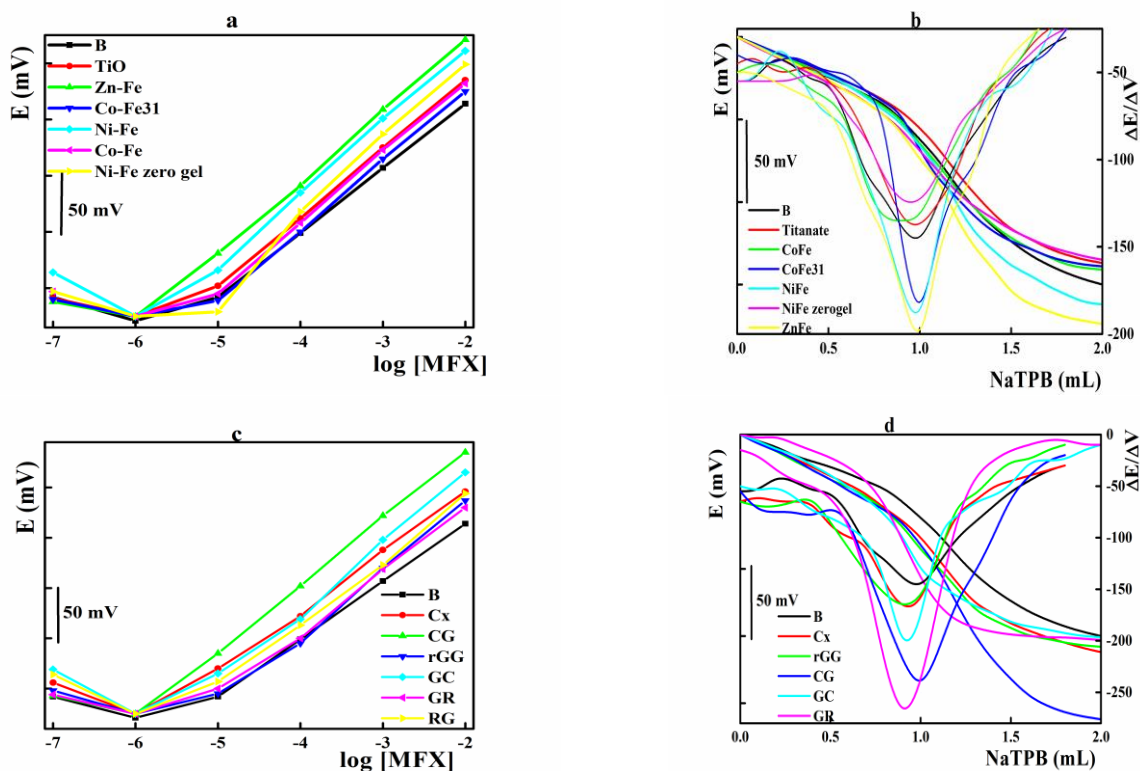
Figure 4 showed the calibration graphs and potentiometric titration curves of sensors fabricated with the aforementioned plasticizers. The performances were improved for electrodes plasticized with highly polar plasticizer (Nernstian slopes were 57.1 ± 2.9 and 59.1 ± 1.9 mV per decade for *o*-NPOE and *f*-PNPE, respectively). Other plasticizers showed lower Nernstian slope and limited sensitivity.

Potentiometric titration process of MFX with NaTPB was carried out using sensors contained different plasticizers (Fig. 3b). The results showed that *f*-PNPE and *o*-NPOE gave the highest potential jump depending on their dielectric constants compared with other plasticizers and selected for the following studies.

3.1.4. Effect of nanomaterial

Nanomaterials promote the transduction of chemical signal to electrical signal within the sensor matrix which in turn improves the sensor performance [54, 55]. In the present work different families of nanomaterials were incorporated within the sensing membrane matrix including metal/metal oxide nanoparticles (Co/Fe, Ni/Fe, Ni/Fe zero gel, Zn/Fe and TiO₂ nanotubes), carbon materials (Cx, CG, GC, GR and rG) and carbon nanotubes (SWCNTs, MWCNTs and synthetic CNTs).

From the studied metal nanoparticles (Fig. 5a, b), Zn/Fe nanocomposite showed the highest Nernstian slope value (62.0 ± 1.4 mV decade⁻¹) compared with the blank and other tested metal nanoparticles. The same concept was also sustained from the potentiometric titration of MFX with NaTPB applying sensors modified with different metal nanoparticles where Zn/Fe nanocomposite was the best.



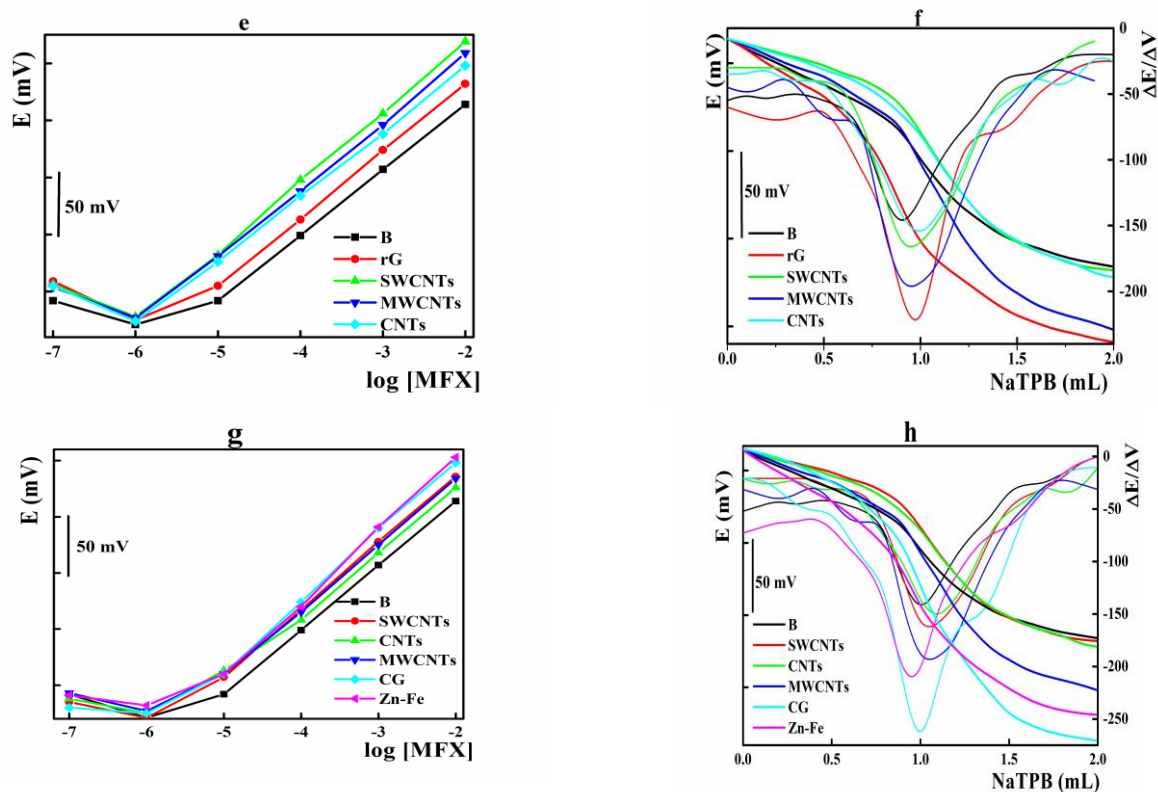


Figure 5. Effect of the different nanomaterials on a, c, e, g) MFx sensor performance; b, d, f, h) potentiometric titration of 1 mL of 10^{-2} mol L $^{-1}$ MFx with 10^{-2} mol L $^{-1}$ NaTPB solution.

Moreover, among carbon materials including carbon gel, Cx, rG, glassy carbon, and graphite sheet, the carbon gel showed the highest electrode performance under the direct potentiometric measurements (Nernstian response was 62.7 ± 0.9 mV decade $^{-1}$) and potentiometric titration mode with total potential jump ($\Delta E = 212$ mV and $\Delta E/\Delta V = 250$ mV mL $^{-1}$) which is much higher than other tested electrode (Fig. 5 c, d). The performances of Zn/Fe and carbon gel based electrodes were compared with that incorporated with carbon nanotubes either SWCNTs or MWCNTs (Fig. 5 g, h). Carbon gel and Zn/Fe still showed superior performance compared carbon nanotubes. In conclusion, sensing membranes containing carbon gel will be selected for the following studies.

3.4. Sensors performance

The fabricated sensors based on 2,3,6-tri-O-methyl- β -cyclodextrin as molecular recognition element in presence of carbon xerogel nanomaterials showed improved sensitivity and selectivity towards meclufenoxate ion (Table 2 and Fig. 6). According to the IUPAC recommendation the cited sensors showed cationic Nernstian compliance of 62.7 ± 0.9 mV decade $^{-1}$ in the MFx concentration range from 10^{-6} to 10^{-2} mol L $^{-1}$ with a detection limit 7×10^{-7} mol L $^{-1}$.

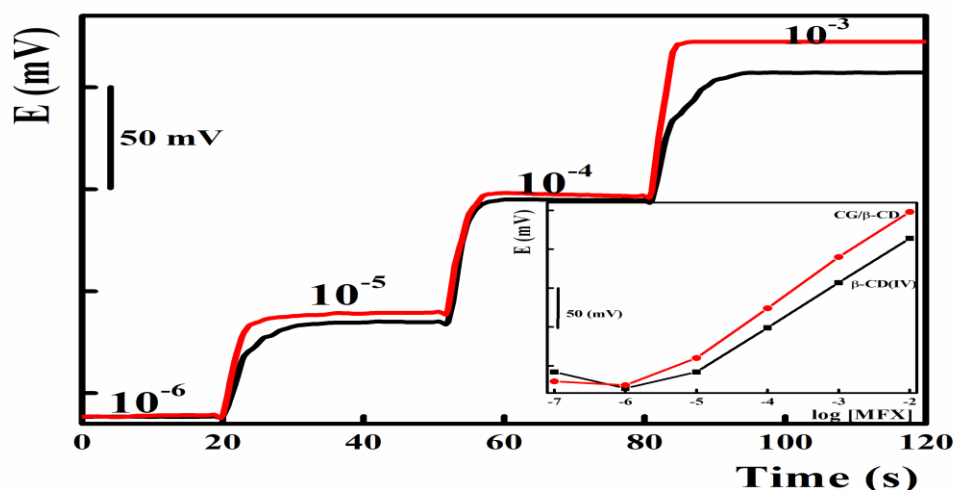


Figure 6. Dynamic response time of different MFX sensors

Table 2. Analytical performances of different meclfenoxate screen printed sensors

Sensors	SPE	SPE/CG/β-CD	
		Batch	FIA
Concentration range (molL ⁻¹)	10 ⁻⁵ -10 ⁻²	10 ⁻⁶ -10 ⁻²	10 ⁻⁶ -10 ⁻²
Slope (mV decade ⁻¹)	57.4 ± 1.0	62.7 ± 0.9	62.0 ± 1.7
R	0.9992	0.9990	0.9994
LOD (molL ⁻¹)	6.0 × 10 ⁻⁶	7.0 × 10 ⁻⁷	1.0 × 10 ⁻⁶
Response time (s)	8	<4	
Preconditioning time (min)	90	<20	
Shelf life time (week)	12	20	

^a Results are the average of five different calibrations..

The sensor fabrication protocol based on screen printing technology offers high fabrication reproducibility. The average Nernstian slope values for 10 sensors fabricated within the same batch were 61.2±1.1 mV decade⁻¹ with standard electrode potential (E^0) equal to 363.6 ± 3.1 mV. Screen printed sensors have all solid state nature showing lifetime of 20 weeks with stable Nernstian response (±2 mV decade⁻¹). Moreover, the fabricated sensors can be contentiously used for 2 weeks without diminishing of their performance.

The MFX electrode response time was estimated by recording the time needed to attain a steady state potential after sudden tenfold increase in the MFX concentration [35]. Carbon gel based electrodes showed spontaneous response (less than 4s) which may be attributed to the synergistic effect between carbon gel nanoparticles and cyclodextrin within the electrode matrix.

The preconditioning time (time needed to get a stable potential reading for a fresh sensor) are limiting factors for application of a newly fabricated sensor. PVC and carbon paste electrodes usually need soaking in the bathing solution over night to attain stable and reproducible potential reading. Solid contact electrodes, such as coated wire electrodes, require shorter preconditioning time but suffer from the poor adhesion of the sensing membrane with metal substrate and the potential drift due to

formation of the undefined water layer between the sensing membrane and conductor [56, 57]. On the other hand, screen printed sensors showed high potential stability due to the co-polymerization between the sensing membrane matrix and the conducting carbon track during the fabrication protocol which prevents the formation of the undefined water layer. Moreover, the presence of carbon xerogel will enhance of the hydrophobicity of the sensing membrane, which contributes to the more stable potential readings [58].

Compared with the previously published MFX sensors, the proposed sensor showed improved performance regarding the sensitivity, lifetime with application in flow injection system and possibility of commercialization (Table 3).

Table 3. Comparison of the analytical parameters of different meclofenoxate electrodes

Analytical parameter	Meclofenoxate Sensors			
	Proposed work	CPE/ β -CD/CNTs [18]	CPE-PMA/CNTs [17]	PVC-TPB [16]
Linear range (mol L ⁻¹)	1×10 ⁻⁶ -1×10 ⁻²	10 ⁻⁶ -10 ⁻²	5×10 ⁻⁵ -10 ⁻²	10 ⁻⁶ -10 ⁻²
Slope (mV decade ⁻¹)	62.7±0.9	57.3±0.5	59.74±0.7	52.73
Detection limit (mol L ⁻¹)	7×10 ⁻⁷	7.6×10 ⁻⁵	5×10 ⁻⁵	10 ⁻⁵
Response time (s)	4	10	4	40
Preconditioning Time	20 min	60 min	24 h	24h
Life time (days)	300	60	36	21 days
FIA	60 S/ h	-----	-----	-----
Titration range (mg)	1.29-12.9	1.29-12.9	8.83-44.13	-----
Large scale production	Applicable	-----	-----	-----

The working pH range is vital operating factors for application of ion selective electrode in pharmaceutical analysis. The dependence of the electrode potential on pH value was investigated at different pH values ranging from 2 to 9. Stable potentials reading was recorded in the pH range from 3 to 8. At higher pH values, dramatic decreasing of the electrode potential was measured due to precipitation of the deprotonated MFX species (pKa is 8.17).

Table 3. Potentiometric selectivity coefficients of MFX-screen printed sensors under batch and FIA conditions.

Interferent	-log $K_{A,B}$				
	Batch ^a	FIA ^b		Batch	
Li ⁺	2.90	3.15	Starch	3.70	-----
NH ₄ ⁺	2.75	3.05	Fructose	3.52	-----
Ca ²⁺	2.40	3.20	Sucrose	3.32	-----
Mg ²⁺	2.60	3.35	Fructose	3.41	-----
Ni ²⁺	3.10	3.40	Glucose	3.35	-----
Co ²⁺	3.23	3.50	Cysteine	2.90	-----
Phosphate	3.00	3.11	Glycine	3.20	-----
Citrate	3.14	3.30	Caffeine	2.70	-----
Degradation product	3.57	3.98			

Sensor selectivity reflects their ability to measure the target analyte in the presence of interfering ions [59]. The presence of excipients in pharmaceutical formulation requires more selectivity of the sensor for accurate analysis. Matched potential method (MPM) was recommended for measuring the selectivity of the ion selective electrodes in case of species with different charged or neutral compounds [60, 61]. Herein, the sensor selectivity toward MFX molecule in presence of other interferents was improved by incorporation of 2,3,6-tri-O-methyl- β -CD to the electrode matrix (Table 3) which may be attributed to the formation of the MFX/ β -CD inclusion complex.

3.4. Analytical Applications

3.4.1. Potentiometric titration

For more analysis accuracy and precision, the potentiometric titration of MFX against NaTPB can be applied using the fabricated sensor as indicator electrode [37].

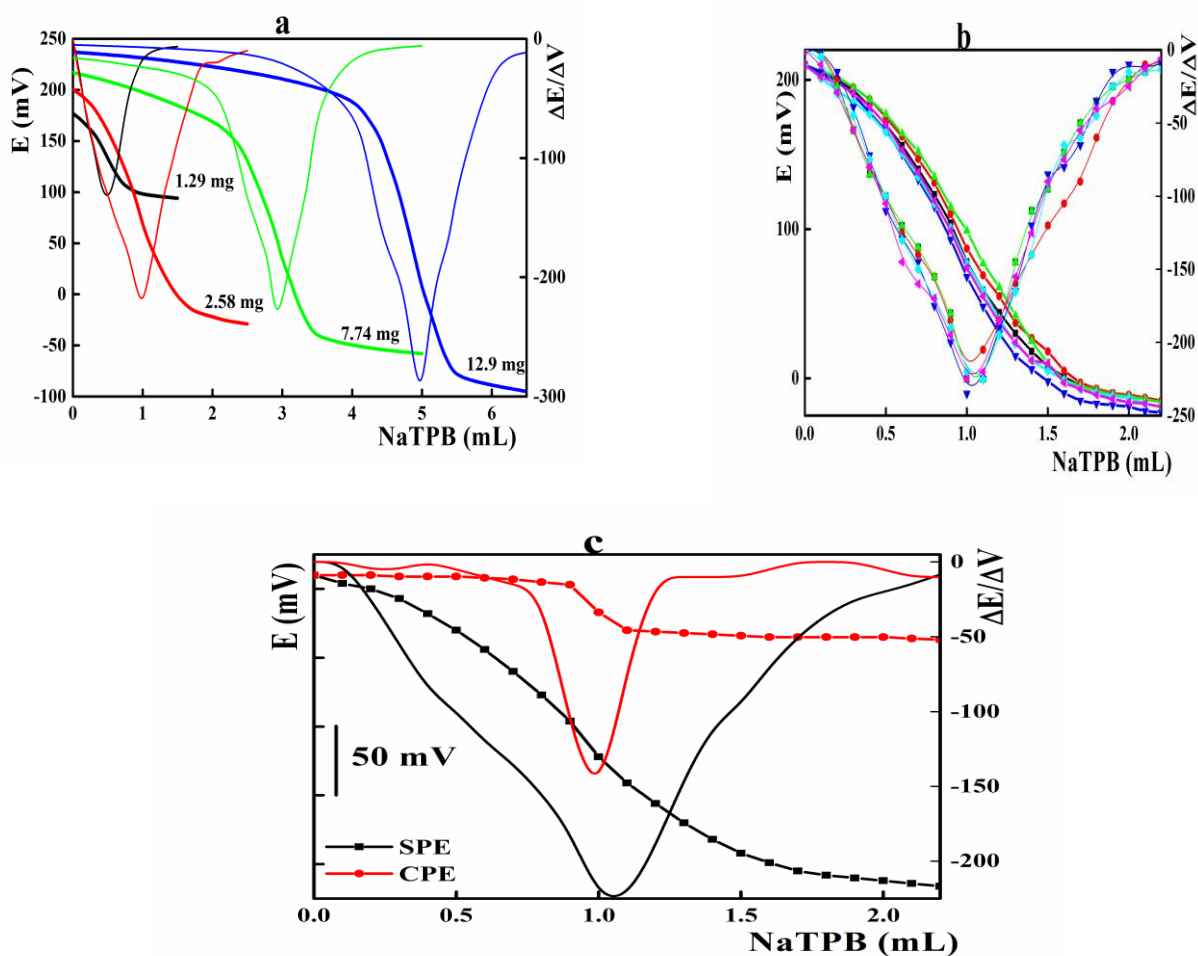


Figure 7. a) Potentiometric titration of different MFX concentrations with NaTPB, b) reproducibility of titration for 1 mL of 10^{-2} mol L^{-1} MFX with 10^{-2} mol L^{-1} NaTPB solution, c) titration of 2.58 mg MFX with 10^{-2} mol L^{-1} NaTPB solution using MFX/SPE and MFX/CPE, respectively.

Titration curves showed considerable potential jumps ranged from 83 to 275 mV for 1.29 to 12.9 mg MFX (Fig. 7a). High reproducibility was achieved for titration of 2.58 mg MFX (7 successive titration process) with average potential jump 229.0 ± 2.2 mV and recovery $101.40 \pm 1.75\%$ (Fig. 7b). It is noteworthy to mention that the present electrode showed improved performance under titration mode (about 5 fold potential jump) compared with the corresponding carbon paste electrodes (Fig. 7c) [18].

3.4.2. Flow Injection Analysis

Seeking for large scale sample analysis and minimizing the analysis errors, potentiometric sensors can be incorporated in flow injection systems [62, 63]. The sensors sensitivity and response time are the two main factors governing the performance of the electrochemical flow injection systems [64]. The fabricated MFX sensors showed stable potential readings and fast response time (4 s) with improved performance, therefore, under FIA system, fast residence time and high sampling output (60 samples h^{-1}) was recorded. Flow injection peaks achieved via injection of 50 μL of MFX solutions covering the concentrations range from 10^{-6} to 10^{-2} mol L^{-1} were illustrated in Figure 8 with Nernstian slope value of 60.0 ± 1.0 mVdecade $^{-1}$.

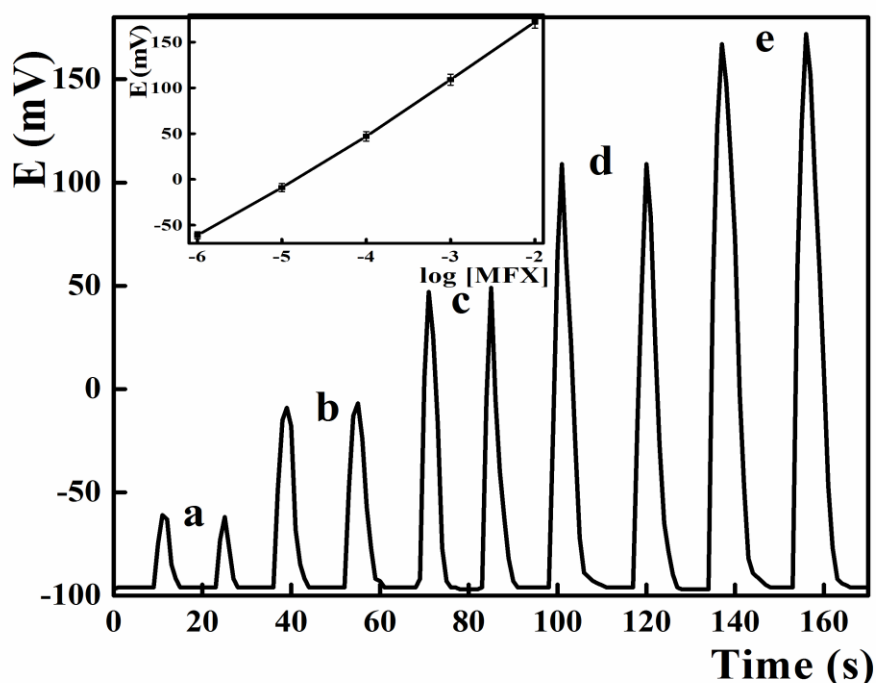


Figure 8. FIA potentiometric determination of MFX using 2,3,6-tri-O-methyl- β -CD/carbon gel based screen printed electrode via injection of 50 μL sample at flow rate 12.6 mL min^{-1} , a to e) 10^{-6} to 10^{-2} mol L^{-1} .

3.4.3. Determination of meclofenoxate in presence of its degradation product

According to El-Bardicy [16], MFX was degraded to p-chloro phenoxy acetic acid and N,N-dimethyl ethanol amine. The second is a volatile compound with a fishy odor while p-chloro phenoxy was precipitated and recrystallized with alcohol.

Due to liberation of the tertiary amine group, which is responsible for potentiometric response and formation of the ion pair [37], the fabricated sensor did not show any potentiometric response towards the p-chloro phenoxy either under direct potentiometric measurement or potentiometric titration against NaTPB. Thus, the proposed β -CD based sensor was applied for potentiometric determination of MFX in presence of its degradation products without any noticeable interference

3.3.4. Sample Analysis

The achieved high sensitivity and selectivity of the fabricated sensors towards MFX suggests their application as efficient tool for meclofenoxate quality control in biological fluids and pharmaceutical formulations with average recoveries in agreement with the reported official method (Table 4).

Table 4. Potentiometric determination of MFX in pharmaceutical preparations and biological fluids

Analytical technique	Taken (μg)	Found			
		Lucidril [®]		Spiked Urine	
		Recovery ^a	RSD ^a	Recovery	RSD
Standard addition	2.58	103.0	2.2	95.2	3.6
	25.8	101.5	1.9	96.4	3.2
	258	99.7	2.5	99.2	2.9
Titration	258	96.2	1.7		
	774	97.9	1.4		
	1290	99.3	1.0		
FIA ^b	5.16	98.7	0.9	95.8	2.7
	51.6	99.2	1.1	98.4	2.1
	516	100.8	1.3	100.7	1.9

^a Mean recovery and relative standard deviations of five determinations

4. CONCLUSION

In this study, the fabrication of an improved disposable potentiometric sensor modified with cyclodextrin and carbon gel as novel nanomaterial for meclofenoxate assay was described. Nernstian compliance of 62.7 ± 0.9 mV decade⁻¹ was obtained in wide MFX concentration range with spontaneous response time and relatively long operational lifetime (20 weeks). The novel sensors were applied for

meclofenoxate analysis in dosage and biological samples in presence of its degradation product with acceptable recoveries comparable to the official methods. Improved performance was achieved compared with other reported MFX sensors (Table 3) regarding the sensitivity, lifetime with application in flow injection system and possibility of commercialization. No interference was detected from the MFX degradation product suggesting the application of this method as stability indicating technique for MFX quality control.

References

1. D. Marcer, S.M. Hopkins, *Age Ageing*, 6 (1977) 123.
2. P.L. Wood, A. Péloquin, *Neuropharmacology*, 21 (1982) 349.
3. J.J. Zou, H.J. Ji, D.W. Wu, J. Yao, Q. Hu, D. Xiao, G.J. Wang, *Clin. Ther.*, 30 (2008) 1651.
4. T. Tsuchihara, F. Tabuchi, *Chem. Pharm. Bull.*, 28 (1980) 779.
5. H. Yang, F.C. Thyron, *J. Liq. Chromatogr. R.T.*, 21 (1998) 1347.
6. T. Meng, M. Zhao, M. Li, F. Chen, *Disi Junyi Daxue Xuebao*, 27 (2006) 1919.
7. L. Jing, C. Yu, Cuixia, Q. Zhang, J. Zhang, J. Zhu, S. Lou, Y. Zhu, *Zhongguo Yaoshi*, 15 (2012) 800.
8. M.S. Moneeb, F. Elgammal, S.M. Sabry, *J. Appl. Pharm. Sci.*, 6 (2016) 1.
9. J. Fecko, *Acta Pol. Pharm.*, 30 (1973) 61.
10. X. Hu, D. Xu, S. Liu, Z. Liu, C. Li, P. Chen, *Anal. Lett.*, 43 (2010) 2125.
11. W. Ma, Y. Zhou, Y. Wang, L. Bao, *Zhongguo Yiyao Gongye Zazhi*, 42 (2011) 57.
12. K. Vytras, in: J. Swarbrick, J.C. Boylan (Eds.), *Encyclopedia of Pharmaceutical Technology*, vol. 12, Marcel Dekker, New York, 1995.
13. S.A. Ozkan, *Electroanalytical methods in pharmaceutical analysis and their validation*, HNB Publishing, New York NY 2011.
14. L. Angnes, *Pharmaceuticals and Personal Care Products, Environmental analysis by electrochemical sensors and biosensors*, Springer (2015), pp. 881-903.
15. S.A. Ozkan, J. Kauffmann, P. Zuman, *Electroanalysis in Biomedical and Pharmaceutical Sciences*, Springer 2016.
16. M.G. El-Bardicy H.M. Lotfy, M.A. El-Sayed, M.F. El-Tarras, *Yakugaku Zasshi*, 127 (2007) 201.
17. R.M. El-Nashar, N.T. Abdel Ghani, S.M. Hassan, *Anal. Chim. Acta*, 730 (2012) 99.
18. M.M. Khalil, A.A. Abdul Aleem, *Egypt. J. Chem.*, 62 (2019) 727.
19. J.P. Metters, R.O. Kadara, C.E. Banks, *Analyst*, 136 (2011) 1067.
20. J.P. Metters, E.P. Randviir, C.E. Banks, *Analyst*, 139 (2014) 5339.
21. E.P. Randviir, D.A. Brownson, J.P. Metters, R.O. Kadara, C.E. Banks, *Phys. Chem. Chem. Phys.*, 16 (2014) 4598.
22. F.E. Galdino, J.P. Smith, S.I. Kwamou, D.K. Kampouris, J. Iniesta, G.C. Smith, J.A. Bonacin, C.E. Banks, *Anal. Chem.*, 87 (2015) 11666.
23. K.C. Honeychurch, J.P. Hart, *Trends Anal. Chem.*, 22 (2003) 456.
24. J.P. Hart, A.P. Crew, E. Crouch, K.C. Honeychurch, R. Pemberton, *Anal. Lett.*, 37 (2007) 789.
25. G. Hughes, K. Westmacott, K.C. Honeychurch, A.P. Crew, R. Pemberton, J.P. Hart, *Biosensors*, 6 (2016) 50.
26. J.P. Hart, A. Crew, E. Crouch, K.C. Honeychurch, R.M. Pemberton, *Screen-printed electrochemical (bio) sensors in biomedical, environmental and industrial applications*, in *Comprehensive Analytical Chemistry*, ed. S. Alegret and A. Merkoçi, Elsevier Amsterdam 2007.
27. A. Abdelwahab, F. Carrasco-Marín, A.F. Pérez-Cadenas, *Materials*, 12 (2019) 2446.
28. M.M. EL-Deeb, W.M.A. El Roubly, A. Abdelwahab, *Electrochim. Acta*, 259 (2018) 77.

29. M.S. Mahmoud, E. Ahmed, A.A. Farghali, A.H. Zaki, N.A.M. Barakat, *Mater. Chem. Phys.*, 217 (2018) 125.
30. S.A.A. Moaty, A.A. Farghali, R. Khaled, *Mater. Sci. Eng.: C*, 68(2016)184.
31. S.A. Abdel Moatya, A.A. Farghali, M. Moussaa, R. Khaled, *J. Taiwan Inst. Chem. E.*, 000 (2016) 1.
32. A.A. Farghali, M. Bahgat, W.M.A. El Roubay, M.H. Khedr, *J. Alloy Compd.*, 555 (2013) 193.
33. E. Khaled, H.N.A. Hassan, G.G. Mohamed, A.A. Seleim, *Drug Test. Anal.*, 2 (2010) 424.
34. E. Khaled, M.S. Kamel, H.N.A. Hassan, H. Abdel-Gawad, Hassan Y. Aboul-Enein, *Talanta*, 119 (2014) 467.
35. R.P. Buck, E. Lindner, *Pure Appl. Chem.*, 66 (1994) 2527.
36. E.W. Baumann, *Anal. Chim. Acta*, 42 (1968) 127.
37. K. Vytras, *Ion Select. Electrode Rev.*, 17 (1985) 77.
38. M.G. El-Bardicy, H.M. Lotfy, M.A. El-Sayed, M.F. El-Tarras, *Yakugaku Zasshi*, 127 (2007)193.
39. E. Weber, *Supramolecular Chemistry II-Host Design and Molecular Recognition*, Springer-Verlag, Berlin Heidelberg, 1995
40. J. Zen, A.S. Kumar, D. Tasi, *Electroanal.*, 15 (2003) 1073.
41. M.R. Ganjali, P. Norouzi, M. Rezapour, F. Faridbod, M.R. Pourjavid, *Sensors*, 6 (2006) 1018.
42. P. Shahgaldian, U. Pieleles, *Sensors*, 6 (2006) 593.
43. G. Astray, C.G. Barreiro, J.C. Mejuto, R.R. Otero, J.S. Gara, *Food Hydrocolloid*, 23 (2009) 1630.
44. T. Steiner, W. Saenger, *Carbohydr. Res.*, 275 (1995) 73.
45. C.J. Easton, S.F. Lincoln, *Modified Cyclodextrins, Scaffolds and Templates for Supramolecular Chemistry*, Imperial College Press, London, 1999
46. H.S. Nalwa, *Nanostructured materials and nanotechnology*, Academic, USA, 2002
47. E. Khaled, H.N.A. Hassan, M.A. Ahmed, R.O. El-Attar, *Electroanal.*, 29 (2017) 975.
48. U. Schaller, E. Bakker, E.J. Pretsch, *Anal. Chem.*, 67 (1995) 3123.
49. U. Schaller, E. Bakker, U.E. Spichiger, E.J.A.C. Pretsch, *Anal. Chem.*, 66 (1994) 391.
50. E. Bakker, P. Bühlmann, E. Pretsch, *Electroanal.*, 11 (1999) 915.
51. K. Vytras, J. Kalous and J. Jezkova, *Egypt. J. Anal. Chem.*, 6 (1997) 107.
52. W.J. Morf, *The principles of ion-selective and of membrane transport*, Elsevier, New York, 1981.
53. H.C. Visser, F. De Jong, D.N. Reinhoudt, *J. Membr. Sci.*, 107 (1995) 267.
54. Z. Spitalsky, D. Tasis, K. Papagelis, C. Galiotis, *Prog. Polym. Sci.*, 35 (2010) 357.
55. A. Merkoc, M. Pumera, X. Lopus, B. Perez, M. Del Valle, S. Alegret, *Trends Anal. Chem.*, 24 (2005) 826.
56. B.P. Nikolskii, E.A. Materova, *Ion-Sel. Electrode Rev.*, 7 (1985) 3.
57. J. Bobacka, T. Lindfords, M. McCarrick, A. Ivaska, A. Lewenstam, *Anal. Chem.*, 67 (1995) 3819.
58. J. Zhu, X. Li, Y. Qin, Y. Zhang, *Sens. Actuat. B Chem.*, 148 (2010) 166.
59. Y. Umezawa, *CRC Handbook of ion-selective electrodes: selectivity coefficients*, CRC press, 1990
60. Y. Umezawa, P. Buhlmann, K. Umezawa, K. Tohda, S. Amemiya, *Pure Appl. Chem.*, 72 (2000) 1851.
61. K. Tohda, D. Dragoie, M. Shibata, Y. Umezawa, *Anal. Sci.*, 17 (2001) 733.
62. A. Danet, L.L. Zamora, J.M. Calatayud, *JFIA.*, 15 (1998) 168.
63. M. Trojanowicz, M. Szewcznska, M. Wcislo, *Electroanal.*, 15 (2003) 347.
64. E. Khaled, M.S. Kamel, H.N.A. Hassan, *JFIA.*, 27 (2010) 20.